Embryonic stem cells develop into functional dopaminergic neurons after transplantation in a Parkinson rat model

Lars M. Björklund*††, Rosario Sánchez-Pernaute*†§, Sangmi Chung*¶, Therese Andersson*¶‖, Iris Yin Ching Chen§, Kevin St. P. McNaught*†, Anna-Liisa Brownell*§, Bruce G. Jenkins§, Claes Wahlestedt‖, Kwang-Soo Kim*¶, and Ole Isacson*†‡**

*Udall Parkinson's Disease Research Center of Excellence, †Neuroregeneration Laboratories, and ¶Molecular Neurobiology Laboratory, McLean Hospital/Harvard Medical School, 115 Mill Street, Belmont, MA 02478; Departments of §Radiology and **Neurology, Massachusetts General Hospital and Program in Neuroscience, Harvard Medical School, Boston, MA 02114; and ‖Karolinska Institute, SE-17177 Stockholm, Sweden

Although implantation of fetal dopamine (DA) neurons can reduce parkinsonism in patients, current methods are rudimentary, and a reliable donor cell source is lacking. We show that transplanting low doses of undifferentiated mouse embryonic stem (ES) cells into the rat striatum results in a proliferation of ES cells into fully differentiated DA neurons. ES cell-derived DA neurons caused gradual and sustained behavioral restoration of DA-mediated motor asymmetry. Behavioral recovery paralleled in vivo positron emission tomography and functional magnetic resonance imaging data demonstrating DA-mediated hemodynamic changes in the striatum and associated brain circuitry. These results demonstrate that transplanted ES cells can develop spontaneously into DA neurons. Such DA neurons can restore cerebral function and behavior in an animal model of Parkinson's disease.

P arkinson's disease (PD) is a degenerative disorder characterized by a loss of midbrain dopamine (DA) neurons with a subsequent reduction in striatal DA (1). Pharmacological treatment with L-DOPA works initially, but reduced efficacy and development of motor complications requires treatment alternatives such as deep brain stimulation and fetal DA neuron transplantation (2). There is evidence both from animal models and clinical investigations showing that fetal DA neurons can produce symptomatic relief (3–6). Technical and ethical difficulties in obtaining sufficient and appropriate donor fetal brain tissue have limited the application of this new therapy.

Previous work showed that DA neurons can be produced in vitro from ventral mesencephalic (VM) precursor cells (7). A problem using expanded fetal VM precursors (7) is the low in vivo survival rate of 3–5% of the grafted DA neurons, which eliminates the actual gain by in vitro cell number expansion compared with fresh (unexpanded) fetal day-12 VM (7, 8).

Embryonic stem (ES) cells have many characteristics required for an optimal cell source for cell-replacement therapy (9, 10). ES cells are self-renewing and multipotent cells derived from the inner cell mass of the preimplantation blastocyst (11). We have shown previously that mouse ES cells transplanted to normal mice or 6-hydroxydopamine (OHDA)-lesioned rats can differentiate spontaneously into tyrosine hydroxylase (TH)-positive and serotonin (5HT)-positive neurons. This differentiation is likely not caused by a specific inductive signal from the host brain, because similar neuronal differentiation occurs after placement in the kidney capsule (11). In our previous study (11), grafts frequently showed heterogeneous morphology and often became very large, disrupting the cytoarchitecture at the implantation site, which prevented the possibility for functional integration. Because neurons develop from ES cells even when implanted outside the central nervous system (11) and ectoderm develops into neural tissue when cell-to-cell communication is disrupted by dissociation of the cells (12–14), we hypothesized that dilution of ES cells into single-cell

suspensions of low ES cell concentrations would result in neuronal development. A low cell concentration decreases ES cell-to-cell contact and increases the influence from the adult host striatum, which in contrast to adult neurogenic regions may restrict cell migration and proliferation, thus allowing default differentiation (15–17) into neurons in this paradigm.

We show that naive ES cells, when grafted in low numbers, develop into normal midbrain-like DA neurons that reduce motor asymmetries and normalize DA presynaptic markers and downstream corticostriatal hemodynamic changes in animal models of PD.

Methods

Propagation and Preparation of ES Cells. The mouse blastocyst-derived ES cell line D3 (wild type) was obtained from the American Type Culture Collection. Undifferentiated ES cells were maintained on gelatin-coated dishes in DMEM (GIBCO/BRL) supplemented with 2 mM glutamine (GIBCO/BRL), 0.001% β-mercaptoethanol, 1× nonessential amino acids (GIBCO/BRL), 10% donor horse serum (HyClone), and human recombinant leukemia inhibitory factor (2,000 units/ml, R & D Systems). Early passage cultures were frozen in 90% horse serum/10% DMSO, and aliquots of cell vials were stored in liquid nitrogen. ES cells were thawed for use and cultured for 2 weeks in the presence of leukemia inhibitory factor. After that the cells were trypsinized (0.05% trypsin-EDTA, GIBCO), resuspended, and seeded at 5×10^6 cells in 15 ml of DMEM in a 100-mm Fisher brand bacteriological grade Petri dish in the absence of leukemia inhibitory factor. During this treatment, horse serum was replaced by 10% FCS (HyClone). ES cells did not adhere to the dish but instead formed small aggregates (embryoid body). The ES cells were incubated for 4 days at 37°C before the cells were transferred to a 15-ml sterile culture tube and allowed to settle, spun at 1,000 rpm in an ICE CENTRA CL 2 centrifuge for 5 min, and then collected and rinsed once in Ca^{2+}- and Mg^{2+}-free Dulbecco's PBS (GIBCO/BRL). After rinsing, Dulbecco's PBS was removed, 1.5 ml of trypsin solution was added, and the cells were incubated for 5 min at 37°C and then triturated

with fire-polished Pasteur pipettes with decreasing aperture size to fully dissociate the cells. Finally, ES cells were spun at 1,000 rpm for 5 min, allowing the trypsin solution to be replaced with 200 μl of culture medium, and the viability and concentration of the ES cells were determined by using a hemocytometer after staining with acridine orange and ethidium bromide.

6-OHDA Lesion and Amphetamine Rotations. All animal studies were performed following National Institutes of Health guidelines and were approved by the Institutional Animal Care and Use Committee at McLean Hospital, Massachusetts General Hospital, and Harvard Medical School. Female Sprague–Dawley rats (200–250 g, Charles River Breeding Laboratories) received unilateral stereotaxic injections of 6-OHDA (Sigma) into the median forebrain bundle as described (18). Coordinates were set according to the atlas of Paxinos and Watson (19).

Lesioned animals were selected for transplantation by estimation of rotational behavior in response to amphetamine (4 mg/kg i.p.). Animals were placed (randomized) into automated rotameter bowls, and left and right full-body turns were monitored by a computerized activity monitor system. Animals showing >500 turns ipsilateral toward the lesioned side after a single dose of amphetamine were considered having >97% striatal dopaminergic lesion (20) and were selected for grafting.

Transplantation Procedures. Preanesthesia [acepromazine (3.3 mg/ kg, PromAce, Fort Dodge, IA) and atropine sulfate (0.2 mg/kg, Phoenix Pharmaceuticals, St. Joseph, MO)] was given i.m. 20 min before 6-OHDA-lesioned animals were anesthetized with ketamine/xylazine (60 mg/kg and 3 mg/kg, respectively, i.m.). Animals then were placed in a Kopf stereotaxic frame (Kopf Instruments, Tujunga, CA). Each animal received an injection of 1.0 μl (0.25 μl/min) of ES cell suspension or vehicle into two sites of the right striatum (from the bregma: anterior 1.0 mm, lateral 3.0 mm, ventral 5.0 and 4.5 mm, incisor bar 0) using a 22-gauge, 10-μl Hamilton syringe. Coordinates were set according to the atlas of Franklin and Paxinos (21). A 2-min waiting period allowed the ES cells to settle before the needle was removed. Animals received 1,000–2,000 ES cells per μl. An i.p. injection of buprenorphine (0.032 mg/kg) was given as postoperative anesthesia. Twenty-five rats received ES cell injections, and 13 rats received sham surgery by injection of vehicle (medium). Six rats showed no graft survival and five rats died before completed behavioral assessment and were found to have teratoma-like tumors at postmortem analysis. A set of five rats that did not receive full behavioral testing was analyzed histologically.

Immunosuppression. To prevent rejection of grafted mouse ES cells, rat hosts (and control animals) received immunosupression by s.c. injections of cyclosporine A (15 mg/kg, Sandimmune, Sandoz Pharmaceutical) diluted in extra virgin oil each day starting with a double-dose injection 1 day before surgery. Ten weeks postgrafting, the dosage was reduced to 10 mg/kg.
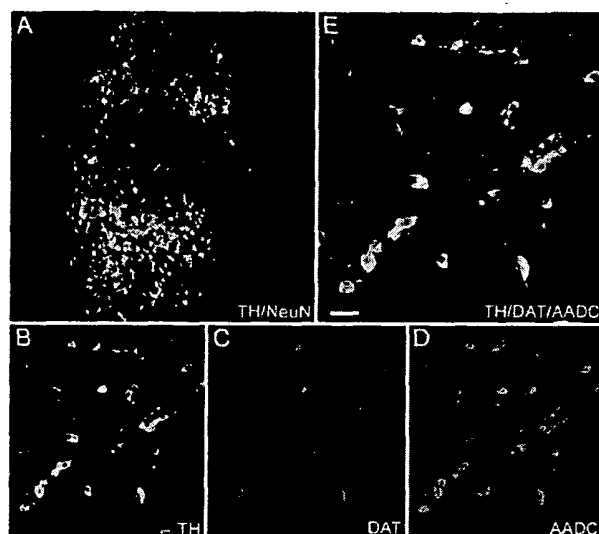
Histological Procedures. After implantation of ES cells (14–16 weeks), animals were anesthetized terminally by an i.p. overdose of pentobarbital (150 mg/kg) perfused intracardially with 100 ml of heparin saline (0.1% heparin in 0.9% saline) followed by 200 ml of paraformaldehyde (4% in PBS). Brains were postfixed for 8 h in the same solution and then equilibrated in sucrose (20% in PBS), sectioned at 40 μm on a freezing microtome, and collected in PBS.

Immunohistochemistry and Cell Counting. Sections were rinsed in PBS, preincubated in 4% normal donkey serum (Jackson ImmunoResearch) for 60 min, and incubated overnight at room temperature in sheep anti-TH (Pel-Freez Biologicals, 1:200), rabbit anti-5HT (Incstar, Stillwater, MN; 1:2,500), rabbit anti-dopamine-β-hydroxylase (1:200), sheep anti-aromatic amino acid decarboxylase

(AADC; 1:200), rat anti-DA transporter (DAT; 1:2,000), mouse anti-neuronal nuclei (NeuN; 1:200), rabbit anti-γ-aminobutyric acid (1:200), mouse anti-glial fibrillary acidic protein (1:150) (all from Chemicon), mouse anti-calbindin (Sigma; 1:1,000), rabbit anti-aldehyde dehydrogenase 2 (a kind gift from R. Lindahl; 1:1,500), rabbit anti-choline acetyltransferase (Roche Molecular Biochemicals; 1:500), mouse anti-proliferating cell nuclear antigen and goat anti-Ki 67 (both from Santa Cruz Biotechnology; 1:100), rat anti-M6 (Hybridoma Bank, Iowa City, Iowa; 1:1,000), and mouse anti-stem cell-specific embryonic antigen 1 (Hybridoma Bank, 2.5 μg/ml) diluted in PBS with 2% normal donkey serum and 0.1% Triton X-100. After rinsing in PBS, sections were incubated in fluorescent-labeled secondary antibodies (Cy2/rhodamine red-X/ Cy5-labeled, raised in donkey; Jackson ImmunoResearch) in PBS with 2% normal donkey serum and 0.1% Triton X-100 for 60 min at room temperature. After rinsing in PBS, sections were mounted onto gelatin-coated slides and coverslipped in gel/mount (Biomeda, Foster City, CA). Fluorescence staining was evaluated by using a Leica TCS-NT laser confocal microscope. Sections used for TH cell counting were stained by using rabbit anti-TH (Pel-Freez Biologicals; 1:500) and standard ABC technique as described (11). Labeling with 4 μg/ml (in PBS) bisbenzimide (Hoechst 33342, Sigma) was performed on floating sections over 2 min, followed by rinsing in PBS. Counting of TH-positive neurons was performed on every sixth section by using a Zeiss Axioplan light microscope with an ×20 lens. Only stained cells with visible dendrites were counted as TH-positive neurons, and the cell counts from serial sections were corrected by using the Abercrombie method (22). The ratio between 5HT neurons and TH neurons was measured on five randomly chosen double-labeled sections per animal.

Statistical Analysis. Rotation scores for ES cell-grafted and control (sham surgery) animals were contrasted by using t tests and, for repeated measures situations, generalized estimating equation (GEE)-based regression modeling methods. The GEE method included robust estimation of standard errors and adjustment for clustering within subjects. GEE was used instead of ordinary ANOVA methods because of missing data for some animals at 5 weeks posttransplantation. However, the missing data did not correlate with the rotation outcome or change in rotations. The Student's t test was used to compare pretransplantation rotational scores (baseline) within each group compared with each separate time point (5, 7, and 9 weeks) posttransplantation. Because post hoc analysis was performed, significance values were corrected by using the Bonferroni method. Differences were considered statistically significant when $P < 0.05$. Exclusion criteria from the transplantation group were absence of surviving graft or tumor-like grafts with typical morphology for mesodermal, endodermal, and epidermal tissue, or graft location outside the striatum. Data are presented as mean $\pm$ SEM. Statistical analysis and data for normal distribution for rotational behavior after lesion and transplantation were performed by using STATA software.

Imaging. All imaging studies were carried out under halothane anesthesia. positron emission tomography (PET) studies were performed by using a high-resolution single-ring tomograph (PCR-I; ref. 23), and serial dynamic acquisitions were performed over 60–90 min by using 5-mm steps. Binding ratios were calculated by using graphically integrated activity in the striatum and cerebellum (reference region) as described (23). MRI studies were performed on a 4.7 General Electric Omega CSI imager (24–26). We used the increased relaxivity with iron-based nanoparticles (27) technique with monocrystalline iron oxide nanocolloid. Using long half-life iron oxide i.v. agents, relative cerebral blood volume (CBV) can be estimated easily, because at steady-state, changes in local tissue relaxivity are directly proportional to changes in local tissue blood volume (28). The use of such agents increases the contrast-to-noise ratio such that at low and intermediate magnetic field
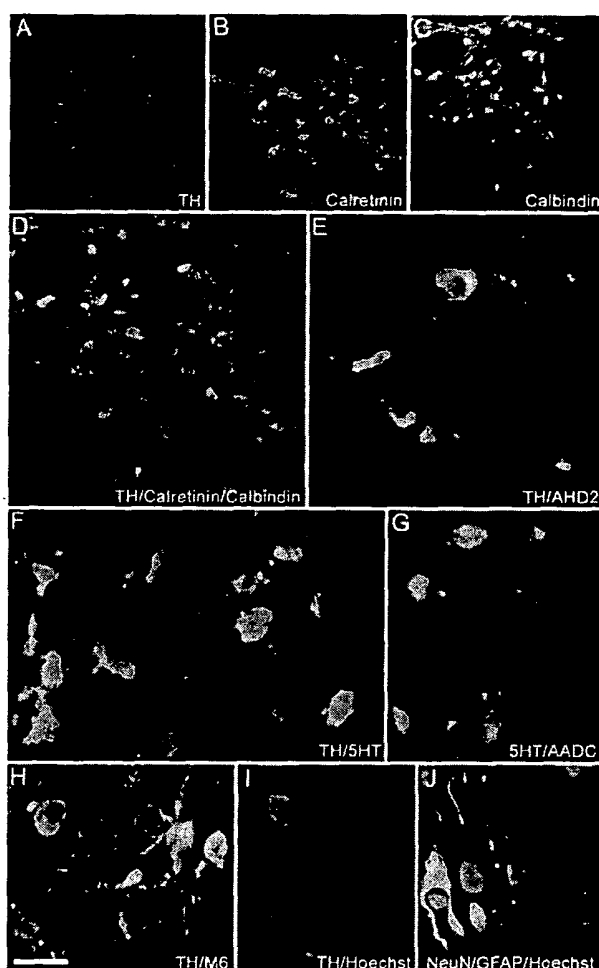
Fig. 1.   Immunohistochemical staining of a graft 16 weeks after implantation of a low concentration (1,000–2,000 cells per μl) of D3 ES cells into adult 6-OHDA lesioned striatum. Numerous TH-positive neurons were found within the graft (A and B, green). All TH-positive profiles coexpressed the neuronal marker NeuN (A, red). TH (B) also was coexpressed with DAT (C, red) and AADC (D, blue), demonstrated by white triple labeling (E). (Scale bars: A, 150 μm; B–D, 50 μm; E, 25 μm.)

strength, CBV provides temporal and spatial resolution sufficient to detect slowly evolving activation induced by pharmacological challenges (29). After the acquisition of 10 baseline images, we injected monocrystalline iron oxide nanocolloid (10 mg/kg) to sensitize the images to relative CBV (rCBV) and collected 10 images as described. Amphetamine (2 mg/kg) then was injected, and images were collected for 90–120 min. Statistical maps were made by using Kolmogorov–Smirnov statistics (24). Changes in signal intensity were converted to rCBV on a pixel-by-pixel basis, color-coded according to statistical significance, and displayed on the anatomical images (24).
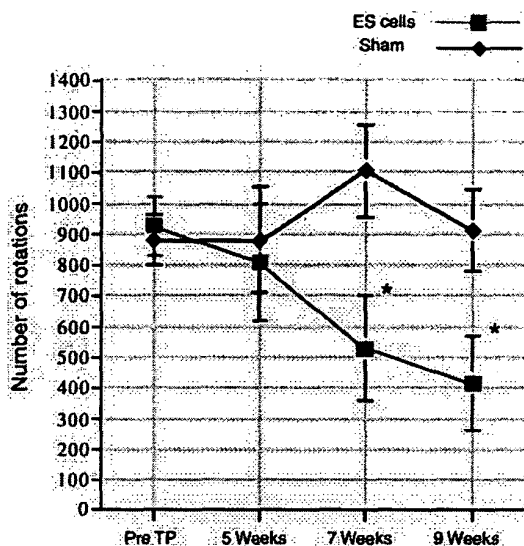
Results

ES Cells Differentiate into Mesencephalic Dopaminergic-Like Phenotypes After Transplantation to the Adult Brain.

We grafted mouse ES cell suspensions of low density (see Methods) into the rat striatum and examined graft markers at 14–16-weeks survival by using immunofluorescence and confocal microscopy. Fourteen animals had grafts located in the striatum. Numerous TH-positive neurons (2,059 ± 626) were identified at the implantation site by colabeling of TH (Fig. 1A, green) and the neuronal marker NeuN (Fig. 1A, red). Dopaminergic neuronal phenotypes were demonstrated by colabeling of DA key proteins such as TH (Fig. 1B), the DAT (Fig. 1C), and AADC (Fig. 1D). ES cell-derived TH-positive neurons coexpressed AADC and DAT (Fig. 1E). Cellular distribution of TH and DAT staining showed very similar patterns (Fig. 1 B and C), whereas AADC-positive cells were found that did not show immunoreactivity against TH or DAT. All TH-positive neurons (Fig. 2A) coexpressed calretinin (Fig. 2 B and D), which normally is coexpressed with TH in both A9 and A10 regions of the ventral midbrain, and some TH-positive neurons coexpressed calbindin (Fig. 2 C and D), which is found primarily in A10 DA neurons. Calbindin also was expressed by host striatal neurons (Fig. 2 C and D) and some non-TH neurons within the grafts. In addition, we found ES cell-derived TH-positive neurons coexpressing the A9 midbrain DA neuron marker aldehyde dehydrogenase 2 (Fig. 2E, yellow coexpression). These findings demonstrate that grafted ES

Fig. 2.   Photomicrograph showing TH-positive neurons (A and D) coexpressing (D) typical midbrain DA neuron markers such as calretinin (B and D) and calbindin (C and D). TH-positive neurons (E, green) also coexpressed the A9 marker aldehyde dehydrogenase 2 (E, yellow coexpression). Numerous 5HT neurons were found in grafts (F, green), and 5HT neurons also coexpressed AADC (G, green, yellow coexpression with 5HT). Grafted mouse ES cell-derived DA neurons (H, yellow, and I, red) were identified by colabeling with mouse-specific antibodies, M6 (H, yellow coexpression with TH), or by mouse-specific intranuclear fluorescent inclusions after Hoechst staining (I, blue). Astrocytes (glial fibrillary acidic protein-positive, J, green) and neurons (NeuN-positive, J, red) show mouse intranuclear fluorescent inclusions (Hoechst, J, blue). (Scale bars: A–C, 100 μm; D, 67 μm; E–J, 20 μm.)
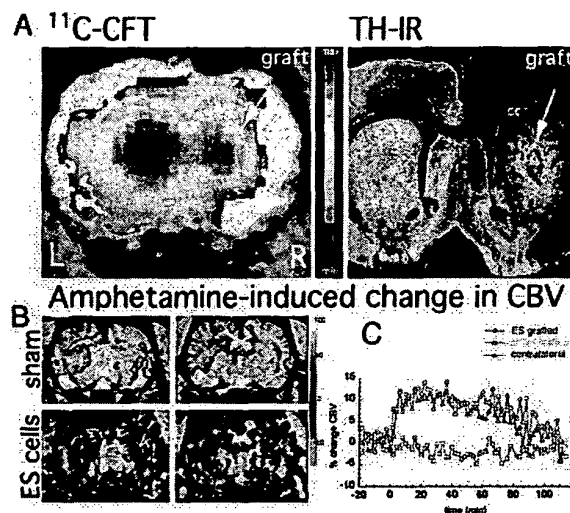
cells differentiate into an adult VM-like DA neuronal phenotype after transplantation in vivo at low cell densities and doses. The presence of numerous AADC-positive neurons negative for TH or DAT can be explained by the presence of 5HT neurons (Fig. 2F, green, and 2G, red) that also coexpress AADC (Fig. 2G, green and yellow coexpression with 5HT). The ratio between DA and 5HT neurons within the grafts was ≈2:1. All TH- and 5HT-positive cells expressed the neuronal marker NeuN. To determine whether some of the TH-positive neurons in the grafts were noradrenergic we performed double labeling for TH and DA β-hydroxylase and we did not find any DA β-hydroxylase-positive neurons within the grafts (data not shown and ref. 11). In addition to monoaminergic neurons, grafts also contained a small number of γ-aminobutyric acid neurons as well as choline acetyltransferase neurons (data not

ES cells ———■———
Sham ———◆———

Fig. 3. Rotational behavior in response to amphetamine (4 mg/kg) was tested pretransplantation (pre TP) and at 5, 7, and 9 weeks postgrafting. A significant decrease in absolute numbers of amphetamine-induced turning was seen in animals with ES cell neural DA grafts in the striatum ($n = 9$) compared with control animals that received sham surgery ($n = 13$). Animals with sham surgery showed no change in rotational score over time ($t = 1.51, P = 0.14$). In contrast, animals with ES cell-derived neural grafts showed a significant reduction in rotations over time ($t = -5.16, P < 0.001$). We then examined at what time point rotational decrease was reduced significantly compared with pretransplantation scores. Because we performed post hoc comparisons, Bonferroni correction was applied to the significance criterion (adjusted criterion, $P = 0.05/3 = 0.017$). At 5 weeks postgrafting, ES cell-grafted animals showed no significant difference in rotations compared with pretransplantation scores (808 ± 188 vs. 924 ± 93 rotations, $t = -0.62, P = 0.58$). However, a clear and significant difference was evident at 7 weeks (530 ± 170 vs. 924 ± 93 rotations, $t = -3.66, P = 0.0064$) and further at 9 weeks (413 ± 154 vs. 924 ± 93 rotations, $t = -4.30, P = 0.0026$). *, $P < 0.01$.

Fig. 4. (A) By using PET and the specific DAT ligand [^{11}C]CFT, we identified specific binding in the right grafted striatum, as shown in this brain slice (A, Left) acquired 26 min after injection of the ligand into the tail vein (acquisition time was 15 sec). Color-coded (activity) PET images were overlaid with MRI images for anatomical localization. The increase in [^{11}C]CFT binding in the right striatum was correlated with the postmortem presence of TH-immunoreactive (IR) neurons in the graft (A, Right). (B) Neuronal activation mediated by DA release in response to amphetamine (2 mg/kg) was restored in animals receiving ES grafts. Color-coded maps of the percentage of change in rCBV are shown at two striatal levels for control (Upper) and an ES cell-derived DA graft (Lower). A 6-OHDA lesion results in a complete absence of CBV response to amphetamine on striatum and cortex ipsilateral to the lesion (Upper). Recovery of signal change in motor and somatosensory cortex (arrows) and to a minor extent in the striatum was observed only in ES-grafted animals. (C) Graphic representation of signal changes over time in the same animal shown in B. The response on the grafted (red line) and normal (blue line) striata was similar in magnitude and time course, whereas no changes were observed in sham-grafted animals (green line). Baseline was collected for 10 min before and 10 min after monocrystalline iron oxide nanocolloid injection, and amphetamine was injected at time 0. cc, corpus callosum.

shown). DA neurons in the rat striatum (Fig. 2H, yellow, and 2I, red) were labeled by the M6 mouse-specific antibody (Fig. 2H, yellow coexpression; ref. 30) and could be identified also by mouse-specific intranuclear fluorescent bodies after labeling with bisbenzimide (Hoechst; ref. 31; Fig. 2I), indicating that they were derived from the implanted mouse ES cells. Five animals were killed because of sickness before the endpoint of the study. These animals had developed teratoma-like structures at the implantation site. However, in all other animals with surviving grafts ($n = 14$), terminal differentiation into a stable nondividing neuronal phenotype was consistent with absence of staining against proliferating cellular nuclear antigen or the proliferation marker Ki 67 in the differentiated neuronal graft. We found numerous astrocytes stained for the astrocyte marker glial fibrillary acidic protein within the grafts. These glial fibrillary acidic protein-positive astrocytes originated both from the host and the grafted ES cells as indicated by the absence or presence of colabeling with mouse-specific nuclear Hoechst labeling (Fig. 2J). We also stained the grafts for the mesodermal marker desmin and myosin and for the epithelial marker keratin. We found that three grafts, in addition to a majority of neural cells, had scattered cells or smaller pockets of cells that were desmin/myosin- or keratin-positive (data not shown). Six grafted rats did not have surviving ES cell grafts. We believe that this may be because of the grafting of very low numbers of cells, general technical issues of brain transplantation, or the possibility of immediate graft rejection (7, 32, 33).

Functional Recovery of Amphetamine-Induced Motor Asymmetry in a Rat Model of PD. 6-OHDA-lesioned animals were selected for transplantation by quantification of rotational behavior in response

to amphetamine (20). The rotational response to amphetamine was examined at 5, 7, and 9 weeks posttransplantation (Fig. 3). Animals with ES cell-derived DA neurons ($n = 9$) showed recovery over time from amphetamine-induced turning behavior, whereas control (sham surgery) animals ($n = 13$) did not ($z = 3.87, P < 0.001$). Importantly, the decrease in rotational scores was gradual (Fig. 3), and animals with ES cell-derived DA neurons showed a significant decrease in rotations from pretransplantation values at 7 weeks (924 ± 93 vs. 530 ± 170 rotations, $P < 0.01$) and 9 weeks (924 ± 93 vs. 413 ± 154 rotations, $P < 0.01$). Similar significant differences were obtained in measures of the percentage of change in rotations.

Functional Imaging of ES Cell-Derived DA Neurons. We used PET and carbon-11-labeled 2β-carbomethoxy-3β-(4-fluorophenyl) tropane ([^{11}C]CFT) to obtain parallel evidence of DA cell differentiation in vivo. By using animals showing behavioral recovery of rotational asymmetry at 9 weeks after implantation of ES cells, we found an increase in [^{11}C]CFT binding in the grafted striatum of 75–90% ($n = 3$) of the intact side (Fig. 4A), whereas markedly less specific activity (<25% of intact side) was found in sham controls ($n = 2$). We have shown previously that 6-OHDA lesions reduce CFT binding to 15–35% of the intact rat striatum corresponding to the histological extent of DA denervation (23) and that fetal VM-cell DA grafts can restore the signal (whereas no changes are observed after transplantation of non-DA cells from the dorsal mesencephalon; ref. 23). These functional effects by ES cell-derived DA neurons are consistent with behavioral recovery after implantation

of fetal DA neurons that occurs when [¹¹C]CFT binding is increased to 75% of normal [¹¹C]CFT levels (23).

PD patients with implanted fetal DA neurons show continuous symptomatic improvements even after DA storage capacity in the striatum (measured by ¹⁸F-DOPA PET) and response to DA-releasing agents has reached a plateau (6, 32). This result is likely caused by a gradual functional integration of grafted DA neurons with the host circuitry (6). To study whether such functional integration seen in patients also occurs between ES cell-derived DA neurons and the host brain, we performed functional MRI after an amphetamine challenge (25). Variations in neuronal activity affect the cerebral oxygen consumption rate that can be measured through MRI evaluation of rCBV (29). DA release in response to amphetamine induces a specific and significant increase in rCBV in the corticostriatal circuitry, which is coupled to neuronal metabolism. This hemodynamic response is absent after 6-OHDA lesion (25). ES cell-grafted animals ($n = 4$) had a robust activation in response to amphetamine in the grafted striatum and ipsilateral sensorimotor cortex. Significant signal changes in these areas were at similar magnitude to those obtained in the contralateral (non-lesioned) hemisphere (Fig. 4 *B* and *C*). Control animals (sham surgery, $n = 3$) had no response (i.e., signal change, Fig. 4 *B* and *C*, green line). These data support the interpretation of ES cells that become appropriate DA neurons that integrate functionally within the host brain.

Discussion

This investigation demonstrates that DA neurons can develop *in situ* from implanted naive ES cells. In an experimental model of PD, these DA neurons reinnervate the host brain, reduce motor asymmetry, and restore physiological functional MRI response to DA-releasing agents.

It is interesting that the time course observed here of recovered response to amphetamine corresponds with the cell donor species' own developmental rate (correlates with length of gestational period). Behavioral recovery after transplantation of postmitotic mouse or rat fetal DA donor cells typically occurs by 4–5 weeks after implantation surgery, whereas for pig or human donor cells from the same relative fetal region, recovery occurs between 8 and 20 weeks (34). Initiation of behavioral recovery in this study by 5–7 weeks is expected given the additional week of *in vivo* development compared with postmitotic rodent fetal DA cells. This result is consistent with our preliminary findings that implanted ES cells gradually lose expression of early embryonic markers such as the stem cell-specific embryonic antigen 1, and TH-positive neurons start to appear within the ES cell grafts around day 14 postimplantation (L.M.B. and O.I., unpublished results). The most direct interpretation of the reduced motor asymmetry observed in our study therefore is that amphetamine caused sufficient DA release from mouse ES cell-derived neurons.

In a preliminary study ($n = 8$) using a methodology for L-DOPA-induced dyskinesias (35), five rats with surviving DA grafts had either a reduction of L-DOPA-induced dyskinesias or no change (K.P.M. and O.I., unpublished observations). Such improvement also has been observed after grafting fetal DA neurons (35). This result supports the notion that functional DA grafts do not generate abnormal DA responses by themselves but rather reduce the dyskinesias (3, 32, 35).

Implanted ES cells primarily developed into neural grafts with high numbers of mature ventral midbrain-like DA neurons identified by markers such as TH, AADC, DAT, aldehyde dehydrogenase 2, calretinin, and calbindin, normally present in adult A9 and A10 DA neurons (36–38). In addition to DA neurons, the differentiated ES cell grafts developed numerous 5HT neurons. It is not known how these 5HT neurons will affect the functional properties of the differentiated striatal ES cell grafts. 5HT has been shown to increase synaptic DA release from DA terminals in striatum (39, 40), indicating that the presence of 5HT neurons in our grafts may

be beneficial for DA release. It is important to note that functional fetal VM grafts are not pure DA neuronal grafts, and they contain ≈20% DA neurons (41, 42). The functionality of ES cell-derived DA neurons in the present study is at least equal to that seen with transplantation of postmitotic DA midbrain fetal neurons (23, 34, 35, 41, 42).

Functional neuroimaging is a valuable tool for *in vivo* assessment of DA differentiation, graft survival, and functional integration (5, 6, 25, 43). PET imaging of presynaptic markers such as fluoro-DOPA, fluoro-metatyrosine, or CFT is used to determine whether implanted cells *in vivo* have the molecular machinery necessary for DA synthesis and/or storage. By using *in vivo* imaging, we found that ES cells developed into DA neurons expressing a highly specific phenotypic marker, consistent with postmortem dopaminergic immunoanalyses. The histological finding of a new DA terminal network in the striatum by ES cells with functional capacity for DA handling matched the finding of reversal of motor asymmetry. Graft-derived DA neurons need to establish functional connections to restore motor performance. This restoration is accomplished through a gradual integration and development of synaptic connectivity, which most likely is responsible for the protracted course of symptomatic improvement observed in patients receiving fetal grafts (5, 6). Activation of DA neurons by specific tasks or pharmacological challenges induces metabolic changes that can be measured with PET or functional MRI (5, 6, 24, 25). In this study, we examined the potential of ES cells not only to differentiate into DA neurons but also to integrate within the host brain circuitry and mediate restoration of cortical motor activation by using functional MRI. The presence of a strong hemodynamic response in the ipsilateral sensorimotor cortex implies that the amphetamine-induced release of DA from grafted cells influenced striatocortical neurotransmission. In summary, our *in vivo* experiments show that ES cells can differentiate into DA neurons and become integrated within the host circuitry mediating functional recovery.

Based on our own observations that grafts resulting from implantation of high concentrations of ES cells often developed into cells originating from all germ layers (11), we hypothesized that diluting epidermal or other germ layer-inducing signals and cell–cell contacts would result in facilitated neuronal differentiation. The application of low doses of ES cells resulted in neuronal DA-containing grafts, which is consistent with the theory of neuronal fate as a default pathway (11, 15–17). During early development, ectodermal cells in the developing embryo either become epidermal or neural. Certain regions such as the Spemann organizer (44) in amphibians and the Node in mice (45) have important roles in the induction of neurons from the ectoderm. Molecules such as noggin (46), follistatin (47), Xnr 3 (48), cerberus (49), and chordin (50) are secreted from the Spemann organizer and are thought to be responsible for the neuralizing effect (47, 48, 51, 52). BMP-4 (bone morphogenetic protein 4) is a powerful inductor of epidermis and an inhibitor of neural fate (53). Disruption of BMP signaling by introduction of dominant-negative versions of these factors or their receptors can lead to neural induction (52, 54, 55), and ectopic neural tissues can be induced in developing mouse embryos after heterotopic grafting of the node (56). Recently, Tropepe *et al.* (17) showed that dilution of ES cell concentration *in vitro* facilitates neuronal differentiation compared with ES cell cultures of higher density. This effect could be mimicked by BMP antagonists such as noggin and cerberus as well as by using ES cells with a targeted null mutation in the *Smad4* gene, a critical intracellular transducer of multiple transforming growth factor-β signaling pathways (17). The reasons for grafted ES cells specifically becoming DA neurons *in vivo* are not known currently. Interestingly, *in vitro* protocols describing the generation of DA neurons from ES cells show similar proportions of DA neurons (30–40% of total neurons) even though cell culture procedures vary significantly (57, 58). In addition, *in vivo* grafting

studies show that DA neurons will develop also when placed in the kidney capsule or cortex (11). These findings support a default DA development pathway (16) from ES cells. Furthermore, because striatum is a target area for DA neurons, it may provide growth factor support that increases the survival of DA neuron compared with other neuronal phenotypes. Our findings of ES cell-derived neurons after implantation into striatum are in contrast to adult or non-ES cell precursors or adult stem cells that mainly differentiate into glial cells in the striatum (59, 60). From adult stem cells, neurons are produced after implantation into adult neurogenic regions such as the subventricular zone and the dentate gyrus of the hippocampus (61). It has been shown also that endogenous adult stem cells can replace damaged neurons in response to injury (62), and recent findings suggest that adult stem cells derived from the ependymal layer can give rise to cells of all germ layers after implantation into developing embryos (63). However, whether the adult stem cells can contribute to functional recovery in disease or degenerative models still is not known.

Given the recent successful isolation of human ES cell lines (64, 65), our findings of efficient ES cell transplantation, expansion, and differentiation into functional DA neurons in the adult brain have implications for ES cells as a donor source for cell therapy in PD.

1. Olanow, C. W. & Tatton, W. G. (2000) *Annu. Rev. Neurosci.* **22**, 123–144.
2. Olanow, C. W. & Obeso, J. A. (2000) *Ann. Neurol.* **47**, 167–178.
3. Freed, C. R., Greene, P. E., Breeze, R. E., Tsai, W. Y., DuMouchel, W., Kao, R., Dillon, S., Winfield, H., Culver, S., Trojanowski, J. Q., Eidelberg, D. & Fahn, S. (2001) *N. Engl. J. Med.* **344**, 710–719.
4. Hauser, R. A., Freeman, T. B., Snow, B. J., Nauert, M., Gauger, L., Kordower, J. H. & Olanow, C. W. (1999) *Arch. Neurol. (Chicago)* **56**, 179–187.
5. Piccini, P., Brooks, D. J., Bjorklund, A., Gunn, R. N., Grasby, P. M., Rimoldi, O., Brundin, P., Hagell, P., Rehncrona, S., Widner, H. & Lindvall, O. (1999) *Nat. Neurosci.* **2**, 1137–1140.
6. Piccini, P., Lindvall, O., Bjorklund, A., Brundin, P., Hagell, P., Ceravolo, R., Oertel, W., Quinn, N., Samuel, M., Rehncrona, S., Widner, H. & Brooks, D. J. (2000) *Ann. Neurol.* **48**, 689–695.
7. Studer, L., Tabar, V. & McKay, R. D. (1998) *Nat. Neurosci.* **1**, 290–295.
8. Brundin, P. & Bjorklund, A. (1998) *Nat. Neurosci.* **1**, 537.
9. Hynes, M. & Rosenthal, A. (2000) *Neuron* **28**, 11–14.
10. Svendsen, C. N. & Smith, A. G. (1999) *Trends Neurosci.* **22**, 357–364.
11. Deacon, T., Dinsmore, J., Costantini, L., Ratliff, J. & Isacson, O. (1998) *Exp. Neurol.* **149**, 28–41.
12. Godsave, S. F. & Slack, J. M. (1989) *Dev. Biol.* **134**, 486–490.
13. Grunz, H. & Tacke, L. (1989) *Cell Differ. Dev.* **28**, 211–217.
14. Sato, S. M. & Sargent, T. D. (1989) *Dev. Biol.* **134**, 263–266.
15. Wilson, P. A. & Hemmati-Brivanlou, A. (1997) *Neuron* **18**, 699–710.
16. Hemmati-Brivanlou, A. & Melton, D. (1997) *Cell* **88**, 13–17.
17. Tropepe, V., Hitoshi, S., Sirard, C., Mak, T. W., Rossant, J. & van der Kooy, D. (2001) *Neuron* **30**, 65–78.
18. Costantini, L. C., Cole, D., Chaturvedi, P. & Isacson, O. (2001) *Eur. J. Neurosci.* **13**, 1085–1092.
19. Paxinos, G. & Watson, C. (1986) *The Rat Brain in Stereotaxic Coordinates* (Academic, San Diego).
20. Ungerstedt, U. & Arbuthnott, G. (1970) *Brain Res.* **24**, 485–493.
21. Franklin, K. B. J. & Paxinos, G. (1997) *The Mouse Brain in Stereotaxic Coordinates* (Academic, San Diego).
22. Abercrombie, M. (1946) *Anat. Rec.* **94**, 239–247.
23. Brownell, A. L., Livni, E., Galpern, W. & Isacson, O. (1998) *Ann. Neurol.* **43**, 387–390.
24. Chen, Y. I., Brownell, A. L., Galpern, W., Isacson, O., Bogdanov, M., Beal, M. F., Livni, E., Rosen, B. R. & Jenkins, B. G. (1999) *NeuroReport* **10**, 2881–2886.
25. Chen, Y. C., Galpern, W. R., Brownell, A. L., Matthews, R. T., Bogdanov, M., Isacson, O., Keltner, J. R., Beal, M. F., Rosen, B. R. & Jenkins, B. G. (1997) *Magn. Reson. Med.* **38**, 389–398.
26. Nguyen, T. V., Brownell, A. L., Chen, I. Y. C., Livni, E., Coyle, J. T., Rosen, B. R., Cavagna, F. & Jenkins, B. G. (2000) *Synapse* **36**, 57–65.
27. Chen, Y.-C. I., Mandeville, J. B., Nguyen, T. V., Talele, A., Cavagna, F. & Jenkins, B. G. (2002) *J. Magn. Res. Imaging* **14**, 517–524.
28. Hamberg, L. M., Boccalini, P., Stranjalis, G., Hunter, G. J., Huang, Z., Halpern, E., Weisskoff, R. M., Moskowitz, M. A. & Rosen, B. R. (1996) *Magn. Reson. Med.* **35**, 168–173.
29. Mandeville, J. B., Jenkins, B. G., Kosofsky, B. E., Moskowitz, M. A., Rosen, B. R. & Marota, J. J. (2001) *Magn. Reson. Med.* **45**, 443–447.
30. Lund, R. D., Chang, F. L. F., Hankin, M. H. & Lagenaur, C. (1985) *Neurosci. Lett.* **61**, 221–226.
31. Cunha, G. R. & Vanderslice, K. D. (1984) *Stain Technol.* **59**, 7–12.
32. Isacson, O., Bjorklund, L. & Pernaute, R. S. (2001) *Nat. Neurosci.* **4**, 553.
33. Dunnett, S. B. & Bjorklund, A. (1997) *Brain Res. Brain Res. Protoc.* **1**, 91–99.
34. Isacson, O. & Deacon, T. W. (1997) *Trends Neurosci.* **20**, 477–482.
35. Lee, C. S., Cenci, M. A., Schulzer, M. & Bjorklund, A. (2000) *Brain* **123**, 1365–1379.
36. Nemoto, C., Hida, T. & Arai, R. (1999) *Brain Res.* **846**, 129–136.
37. Hontanilla, B., Parent, A. & Gimenez-Amaya, J. M. (1997) *Synapse* **25**, 359–367.
38. McCaffery, P. & Drager, U. C. (1994) *Proc. Natl. Acad. Sci. USA* **91**, 7772–7776.
39. Blandina, P., Goldfarb, J., Craddock-Royal, B. & Green, J. P. (1989) *J. Pharmacol. Exp. Ther.* **251**, 803–809.
40. De Deurwaerdere, P., Bonhomme, N., Lucas, G., Le Moal, M. & Spampinato, U. (1996) *J. Neurochem.* **66**, 210–215.
41. Bjorklund, A. & Lindvall, O. (2000) *Nat. Neurosci.* **3**, 537–544.
42. Haque, N. S., LeBlanc, C. J. & Isacson, O. (1997) *Cell Transplant.* **6**, 239–248.
43. Tedroff, J., Pedersen, M., Aquilonius, S. M., Hartvig, P., Jacobsson, G. & Langstrom, B. (1996) *Neurology* **46**, 1430–1436.
44. Spemann, H. & Mangold, H. (1924) *Arch. Mikrosk. Anat. Entwicklungsmech.* **100**, 599–638.
45. Zhou, X., Sasaki, H., Lowe, L., Hogan, B. L. & Kuehn, M. R. (1993) *Nature (London)* **361**, 543–547.
46. Smith, W. C. & Harland, R. M. (1992) *Cell* **70**, 829–840.
47. Hemmati-Brivanlou, A., Kelly, O. G. & Melton, D. A. (1994) *Cell* **77**, 283–295.
48. Hansen, C. S., Marion, C. D., Steele, K., George, S. & Smith, W. C. (1997) *Development (Cambridge, U.K.)* **124**, 483–492.
49. Piccolo, S., Agius, E., Leyns, L., Bhattacharyya, S., Grunz, H., Bouwmeester, T. & De Robertis, E. M. (1999) *Nature (London)* **397**, 707–710.
50. Sasai, Y., Lu, B., Steinbeisser, H., Geissert, D., Gont, L. & De Robertis, E. (1994) *Cell* **79**, 779–790.
51. Lamb, T. M., Knecht, A. K., Smith, W. C., Stachel, S. E., Economides, A. N., Stahl, N., Yancopolous, G. D. & Harland, R. M. (1993) *Science* **262**, 713–718.
52. Sasai, Y., Lu, B., Steinbeisser, H. & De Robertis, E. M. (1995) *Nature (London)* **376**, 333–336.
53. Wilson, P. A. & Hemmati-Brivanlou, A. (1995) *Nature (London)* **376**, 331–333.
54. Hawley, S. H., Wunnenberg-Stapleton, K., Hashimoto, C., Laurent, M. N., Watabe, T., Blumberg, B. W. & Cho, K. W. (1995) *Genes Dev.* **9**, 2923–2935.
55. Xu, R. H., Kim, J., Taira, M., Zhan, S., Sredni, D. & Kung, H. F. (1995) *Biochem. Biophys. Res. Commun.* **212**, 212–219.
56. Beddington, R. S. (1994) *Development (Cambridge, U.K.)* **120**, 613–620.
57. Lee, S. H., Lumelsky, N., Studer, L., Auerbach, J. M. & McKay, R. D. (2000) *Nat. Biotechnol.* **18**, 675–679.
58. Kawasaki, H., Mizuseki, K., Nishikawa, S., Kaneko, S., Kuwana, Y., Nakanishi, S., Nishikawa, S.-I. & Sasai, Y. (2000) *Neuron* **28**, 31–40.
59. Svendsen, C. N., Caldwell, M. A., Shen, J., ter Borg, M. G., Rosser, A. E., Tyers, P., Karmiol, S. & Dunnett, S. B. (1997) *Exp. Neurol.* **148**, 135–146.
60. Fricker, R. A., Carpenter, M. K., Winkler, C., Greco, C., Gates, M. A. & Bjorklund, A. (1999) *J. Neurosci.* **19**, 5990–6005.
61. Gage, F. H. (2000) *Science* **287**, 1433–1438.
62. Magavi, S. S., Leavitt, B. R. & Macklis, J. D. (2000) *Nature (London)* **405**, 951–955.
63. Clarke, D. L., Johansson, C. B., Wilbertz, J., Veress, B., Nilsson, E., Karlstrom, H., Lendahl, U. & Frisen, J. (2000) *Science* **288**, 1660–1663.
64. Thomson, J. A., Itskovitz-Eldor, J., Shapiro, S. S., Waknitz, M. A., Swiergiel, J. J., Marshall, V. S. & Jones, J. M. (1998) *Science* **282**, 1145–1147.
65. Reubinoff, B. E., Pera, M. F., Fong, C. Y., Trounson, A. & Bongso, A. (2000) *Nat. Biotechnol.* **18**, 399–404.

NEUROBIOLOGY